

Spin Crossover-Driven Thermochromic Temperature Sensor for Monitoring Heat Transfer via Image Analysis

Bhart Kumar, Kamalesh Tripathy, Mitradip Bhattacharjee, Sanjit Konar*

Contents:

1. Experimental and characterization details
2. Single crystal X-ray diffraction
3. Powder X-ray diffraction
4. Infra-Red analysis
5. Magnetic susceptibility measurements
6. Image processing
7. Variable temperature solid state UV-Visible spectroscopy
8. Heat flow monitoring
9. Temperature mapping
10. References

1. Experimental and characterization details

Materials

All the reagents are commercially available and used without further purification. *Caution: Iron (II) perchlorate is potentially explosive and was used in small quantities to avoid any explosion.*

Physical Measurements

IR spectra were recorded for all the samples with a PerkinElmer Inc. spectrometer in attenuated-total-reflectance (ATR) mode under ambient conditions. Spectra were recorded at 4 cm^{-1} resolution within a wavelength range of $4000\text{-}400\text{ cm}^{-1}$. **Elemental analyses (CHNS)** were performed using Elementar Micro Vario Cube elemental analyzer. **Powder XRD** patterns were recorded using PANalytical EMPYREAN instrument with $\text{Cu K}\alpha$ radiation. PerkinElmer **TGA 4000** thermogravimetric analyzer was used for the thermogravimetric analysis. With an alumina sample holder and an N_2 flow of 10 mL per minute, the analysis was carried out between 25°C to 800°C at a heating rate of 3°C per minute. The **Differential Scanning Calorimetry (DSC)** study was performed using PerkinElmer, Pyris 6 type DSC 6000 instrument. The data was recorded from -20°C to 60°C at a scan rate of $5\text{K}/\text{min}$. An OPPO Reno6 Pro 5G smartphone was used for capturing sensor images for the study.

Single Crystal X-ray diffraction

A Brüker D8 Venture diffractometer equipped with graphite-monochromated $\text{Mo K}\alpha$ radiation ($\lambda = 0.71073\text{ \AA}$) was deployed for structure determination at various temperatures. The APEX-3 crystallographic software (v2018.1.0, Bruker AXS, Inc.) was used for data processing, integration, and

scaling. Space group determination was done using XPREP. The crystal structures were solved using the SHELXT structure solution programme and subsequently refined with SHELXL¹ integrated with Olex² software.² The non-H atoms were refined anisotropically, whereas the hydrogen atoms were fixed using the riding model.

A summary of crystallographic and refinement details is provided in Table S1.

Magnetic Measurement

Magnetic measurements were performed on a microcrystalline sample using a Quantum Design; MPMS-3 VSM instrument. The magnetic moment for the sample was collected under 10000 Oe DC magnetic field. The magnetic data provided in the work has been corrected for sample holder and diamagnetic corrections.

2. Single crystal X-ray diffraction

Table S1. Crystal data and structure refinement parameters for complex **1**.

Empirical formula	C ₂₀ H ₁₂ FeN ₈ Pt	C ₂₀ H ₁₂ FeN ₈ Pt
Formula weight	615.32	615.32
Temperature/K	270 K	325 K
Crystal system	Monoclinic	Monoclinic
Space group	C2/m	C2/m
a/Å	19.470(17)	19.647(9)
b/Å	7.277(6)	7.477(3)
c/Å	7.161(6)	7.367(3)
α/°	90	90
β/°	94.20(2)	99.791(15)
γ/°	90	90
Volume/Å ³	1012.0(14)	1066.5(8)
Z	2	2
ρ _{calc} g/cm ³	2.019	1.916
μ/mm ⁻¹	7.645	7.255
F(000)	584.0	584.0
Crystal size/mm ³	0.08*0.218*0.242	0.092*0.213*0.253
Radiation	MoK _α (λ = 0.71073)	MoK _α (λ = 0.71073)
2θ range for data collection/°	4.196 to 52.234	5.612 to 58.172
Index ranges	-23 ≤ h ≤ 23, -8 ≤ k ≤ 8, -8 ≤ l ≤ 8	-26 ≤ h ≤ 25, -9 ≤ k ≤ 9, -9 ≤ l ≤ 10
Reflections collected	7424	9249
Independent reflections	1059 [R _{int} = 0.1198, R _{sigma} = 0.0897]	1445 [R _{int} = 0.1054, R _{sigma} = 0.0739]
Data/restraints/parameters	1059/0/83	1445/0/87
Goodness-of-fit on F ²	1.079	1.066
Final R indexes [I >= 2σ(I)]	R1 = 0.0996, wR2 = 0.2407	R1 = 0.0910, wR2 = 0.2123
Final R indexes [all data]	R1 = 0.1195, wR2 = 0.2595	R1 = 0.0975, wR2 = 0.2177
Largest diff. peak/hole / e Å ⁻³	8.76/-3.95	11.57/-3.45
CCDC	2390485	2390486

Table S2. Selected angles, bond length values, parameters of supramolecular contacts and distortion parameters for complex **1**.

Complex	1	1
T (K)	270 K	325 K
spin state	LS	HS
$\langle \text{Fe-N} \rangle_{\text{average}} (\text{\AA})$	1.98	2.16
$V_{\text{oct}}(\text{FeN}_6)(\text{\AA}^3)$	10.36	13.37
$\Sigma [^\circ]$ (Oct. Dist. Parameter)	8.86	6.35
$\Theta [^\circ]$ (Tri. Dist. Parameter)	37.51	20.72
$\zeta [\text{\AA}]$ (Length Dist. Parameter)	0.301	0.156
Fe-N \equiv C / $^\circ$	178.16	175.97
$\pi \cdots \pi$ Interactions (C _{py} ...C _{benz}) (\AA)	3.706	3.775

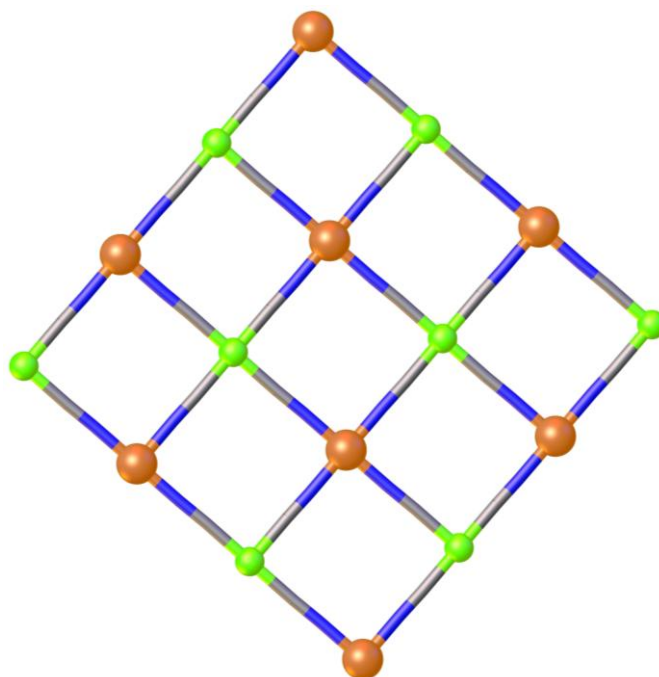


Figure S1. Structural representation of the two-dimensional $\{\text{Fe}^{\text{II}}[\text{Pt}^{\text{II}}(\text{CN})_4]\}_n$ layers lying in the 100-plane (colour Code : Fe - orange, Pt - green spheres).

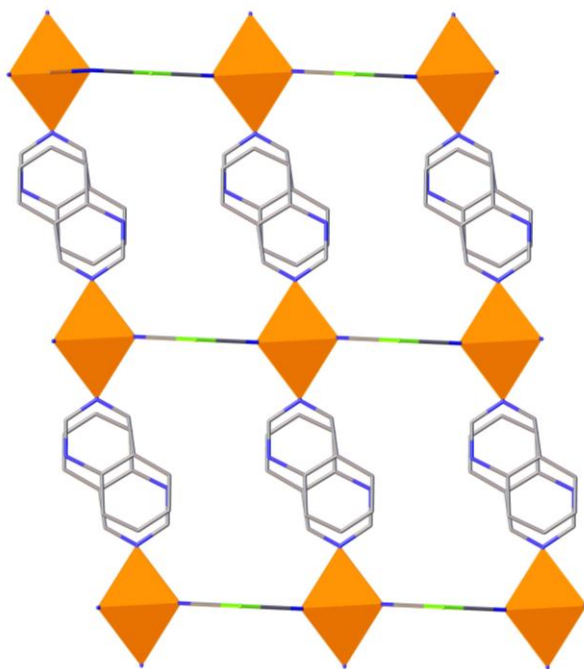


Figure S2. Packing view of complex **1** along 010 plane.

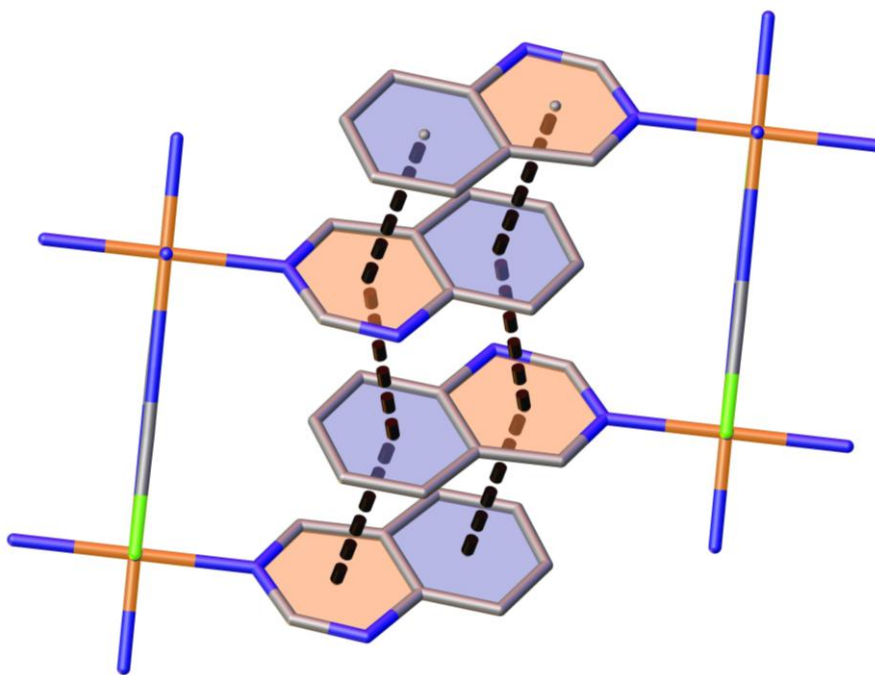


Figure S3. Packing view along 011 plane showing π ... π stacking.

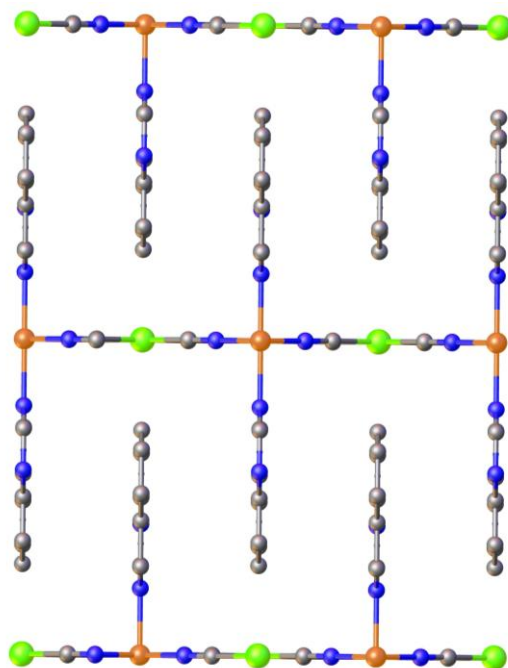


Figure S4. The packing view along the 001 plane shows an almost linear alignment of the $\{\text{Fe}^{\text{II}}[\text{Pt}^{\text{II}}(\text{CN})_4]\}_n$ layers.

3. Powder X-ray diffraction

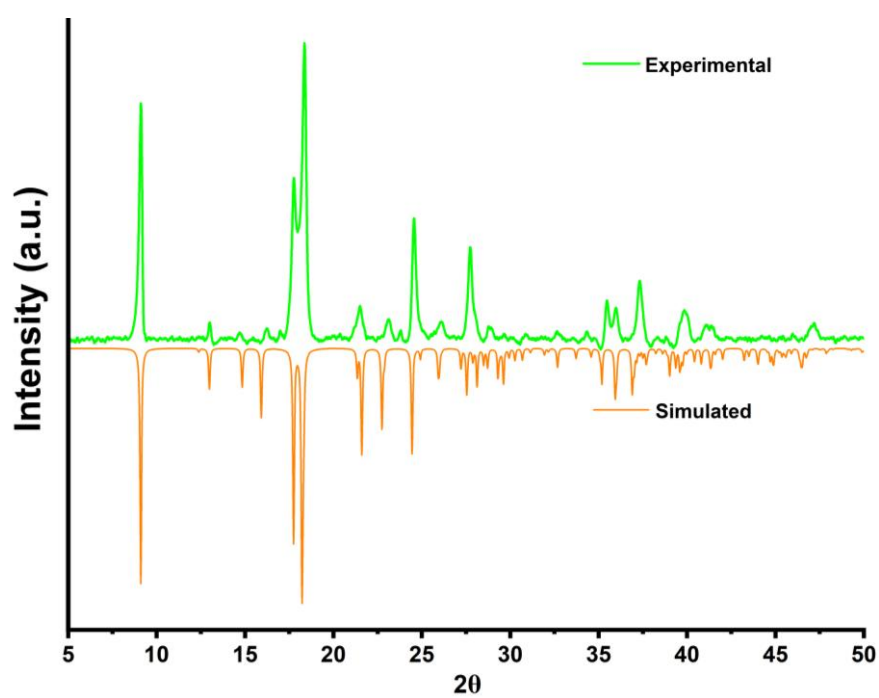


Figure S5. Experimental and simulated PXRD patterns of complex 1.

4. Infra-Red analysis

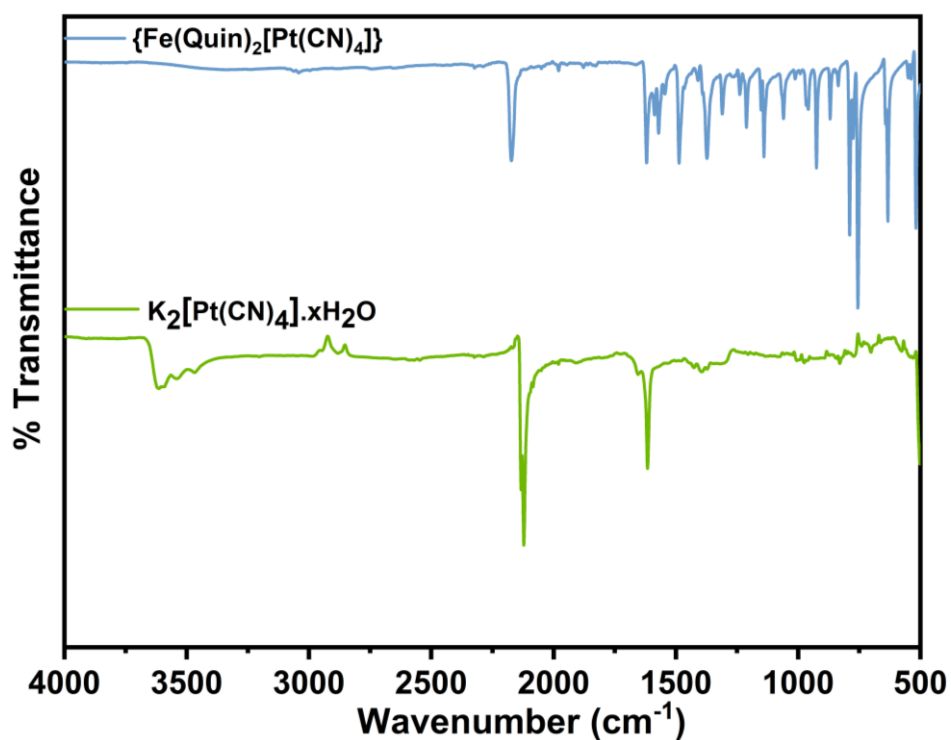


Figure S6. The IR spectra of complex 1 and $\text{K}_2[\text{Pt}(\text{CN})_4] \cdot x\text{H}_2\text{O}$.

5. Magnetic susceptibility measurements

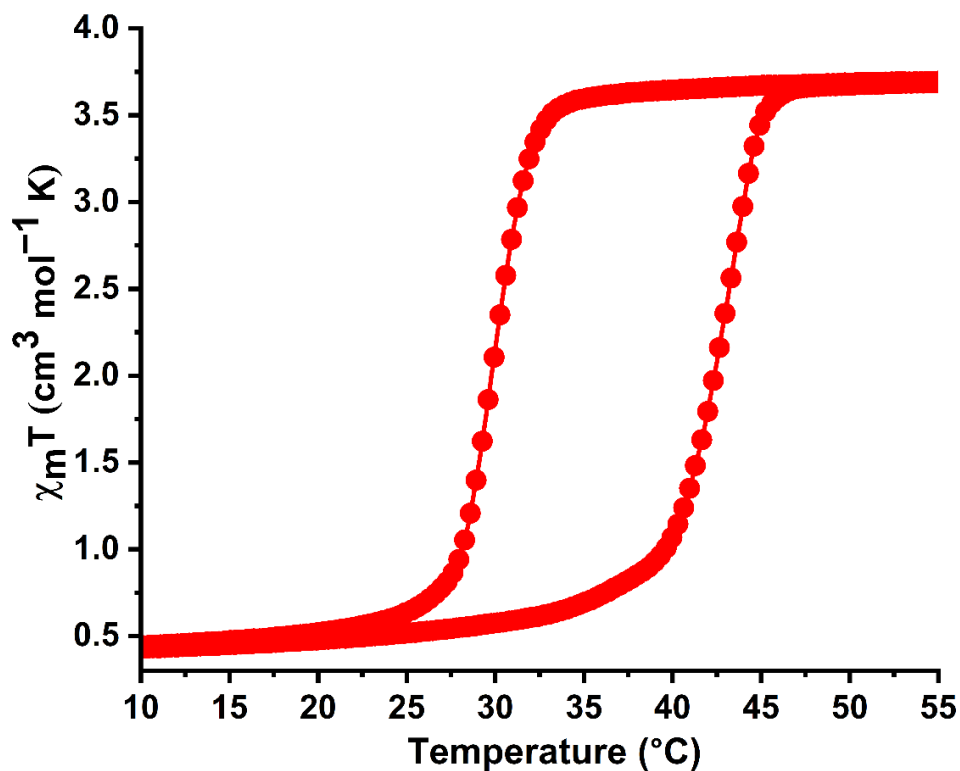


Figure S7. Thermal variation of the $\chi_m T$ product for complex 1 presented in degrees.

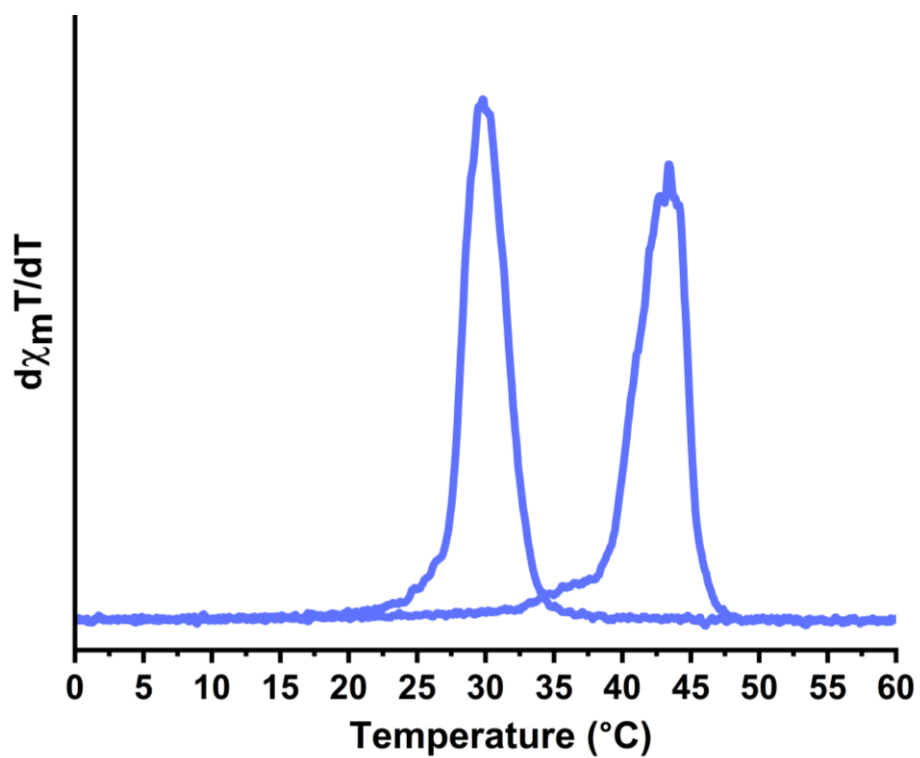


Figure S8. Derivative of $\chi_m T$ vs T plot of complex 1.

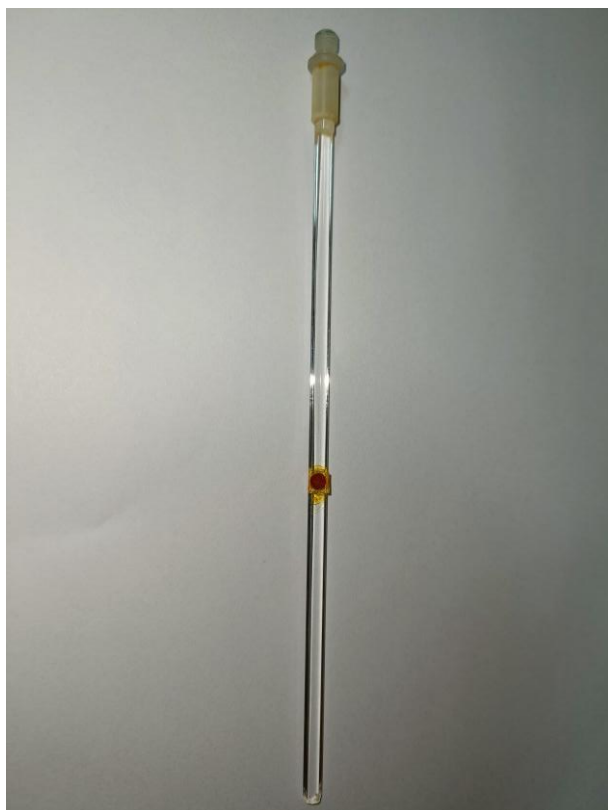


Figure S9. The sensor label stuck to the quartz sample holder for magnetic measurement.

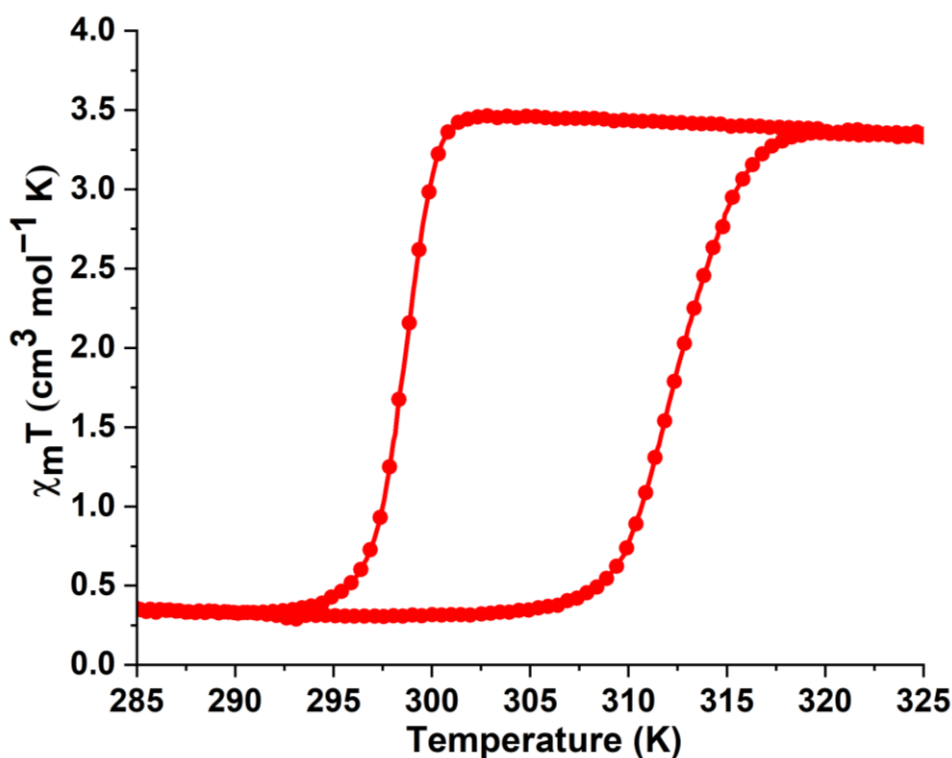


Figure S10. Thermal variation of the $\chi_{M}T$ product for the sensor label.

6. Image processing

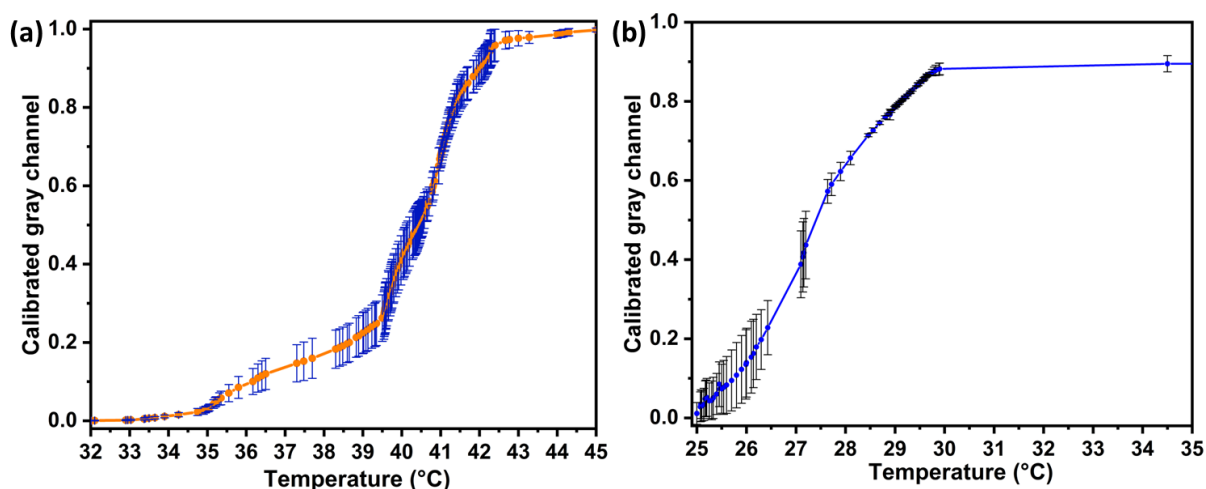


Figure S11. The Gray channel calibration plots for: a) the heating cycle and b) the cooling cycle.

Time response of the sensor :

To measure the transition time for the sensor to switch from low spin to high spin and vice versa, the hotplate was maintained at 60 °C. The sensor was transferred from room temperature (24 °C) to the hotplate surface and the resulting colour change was monitored by the smart phone camera. During the cooling process, the setup was left undisturbed at 24 °C. Further, gray values from the captured images were deduced and plotted against the time axis to determine the transition time (Figure S12). The transition time was calculated as the time taken by the sensor to reach 90% of the maximum normalized G value, starting from 10% of the maximum normalized G value.

(a) Heating

Time corresponding to 10 % of maximum G (0.9) value, $t_1 = 25.65$ sec

Time corresponding to 90 % of maximum G (0.1) value, $t_2 = 48.56$ sec

Response time = $t_2 - t_1 = 22.91$ sec

(b) Cooling

Time corresponding to 90 % of maximum G (0.9) value, $t_1 = 9.03$ sec

Time corresponding to 10 % of maximum G (0.9) value, $t_2 = 27.24$ sec

Response time = $t_2 - t_1 = 18.21$ sec

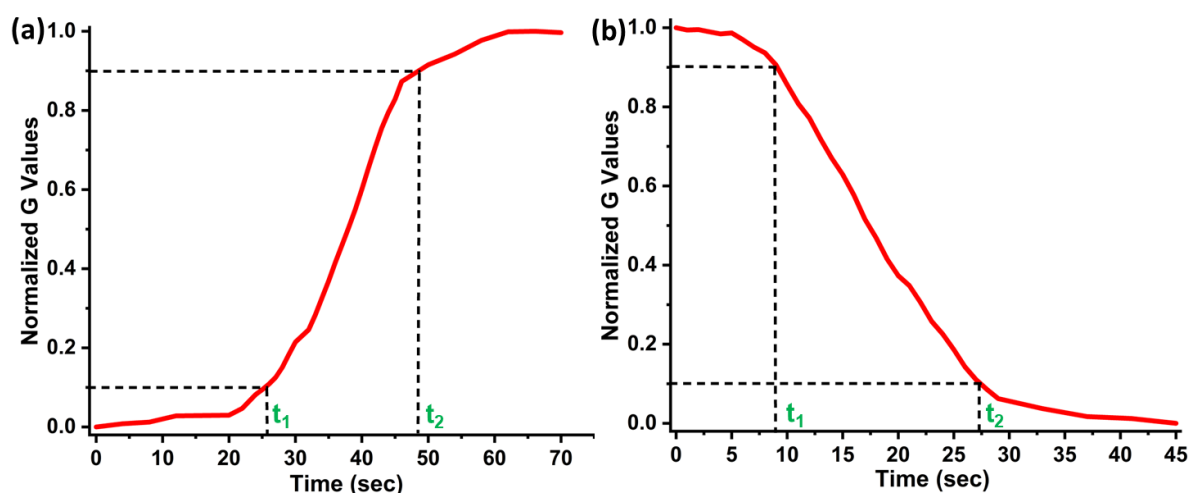


Figure S12. Time response of the sensor for: (a) heating, and (b) cooling cycle.

7. Variable temperature solid state UV-Visible spectroscopy

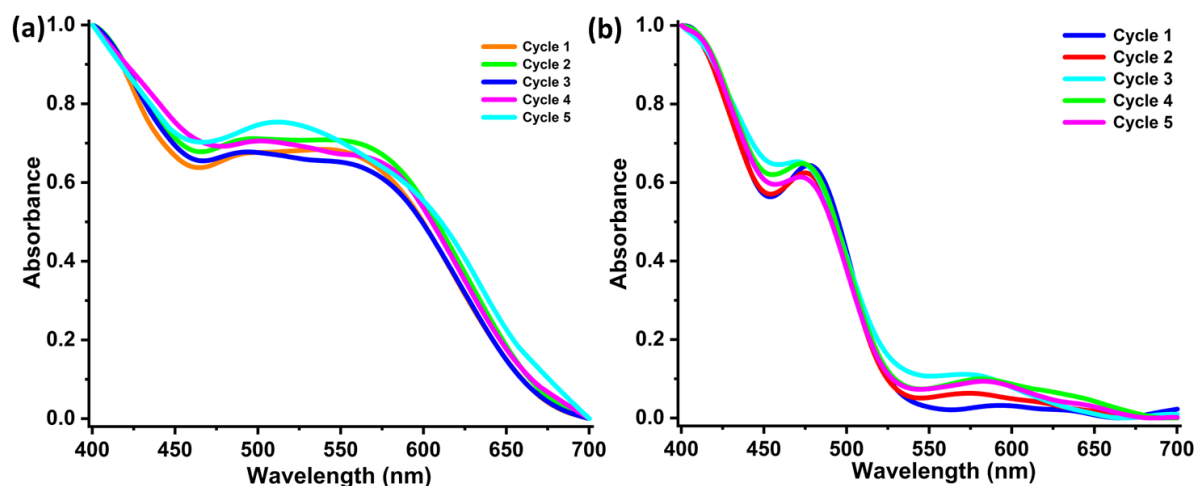


Figure S13. Solid state UV plots confirm the cyclic reversibility of the sensor for (a) heating, and (b) cooling cycles.

Note:- The low spin spectra were collected at 300 K, while for characterising the high spin state, the temperature was maintained at 330 K.

8. Heat flow monitoring

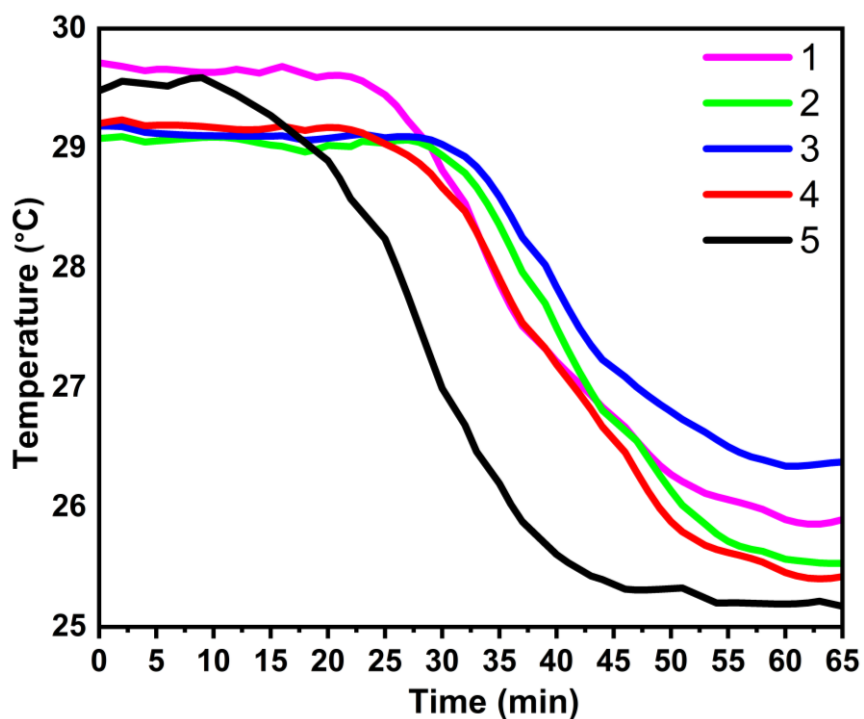


Figure S14. The temperature versus time plot for the cooling cycle, as determined through image processing.

9. Temperature mapping

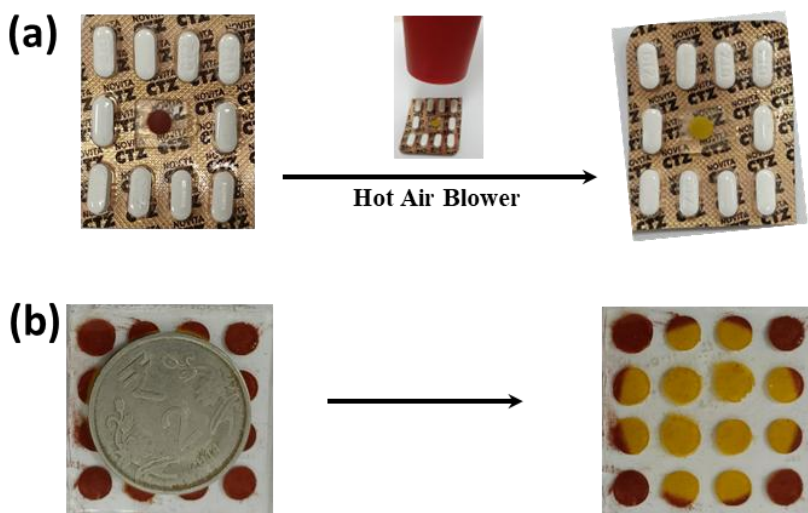


Figure S15. Various applications of the sensor: (a) monitoring threshold storage temperature for life-saving medicines; (b) temperature mapping for disc shaped coin.

Table S3. Temperature values at different times as measured from IR camera and calculated using image analysis

	Time (minutes)	0	30	60	75
Sensor 1	Temperature (°C) (IR, Sensor)	36.65, 37.52	40.56, 40.98	40.97, 41.21	40.58, 41.37
Sensor 2	Temperature (°C) (IR, Sensor)	35.26, 34.48	39.58, 39.99	40.04, 40.33	39.79, 40.55,
Sensor 3	Temperature (°C) (IR, Sensor)	34.47, 34.49	38.69, 39.55	39.43, 39.66	39.49, 39.73
Sensor 4	Temperature (°C) (IR, Sensor)	34.1, 34.21	38.33, 38.31	39.63, 39.66	39.69, 39.70
Sensor 5	Temperature (°C) (IR, Sensor)	33.17, 33.83	37.36, 37.23	38.66, 38.95	38.51, 39.35

10. References

1. G. M. Sheldrick, *A Computer Programme for Crystal Structure Refinement*, 1993.
2. O. V. Dolomanov, L. J. Bourhis, R. J. Gildea, J. A. Howard and H. Puschmann, *J. Appl. Crystallogr.*, 2009, **42**, 339-341.